Wavelet Domain Watermarking Using Maximum Likelihood Detection

Tek Ming Ng† and Hari Krishna Garg
Department of Electrical and Computer Engineering, National University of Singapore, SINGAPORE

Traditionally, digital watermark detection algorithms are based on the correlation between the watermark and the media the watermark is embedded in. Although simple to use, correlation detection is optimal only when the watermark embedding process follows an additive rule and when the medium is drawn from Gaussian distributions. More recent works on watermark detection are based on decision theory. In this article, a maximum likelihood detection scheme based on Bayes' decision theory is proposed for image watermarking in the wavelet transform domain. The decision threshold is derived using the Neyman–Pearson criterion to minimize the missed detection probability subject to a given false alarm probability. The detection performance depends on choosing a probability distribution function (PDF) that can accurately model the distribution of the wavelet transform coefficients. The generalized Gaussian PDF is adopted here. Previously, the Gaussian PDF, which is a special case, has been considered for such detection scheme. Using extensive experimentation, the generalized Gaussian PDF is shown to be a better model.

Journal of Imaging Science and Technology 49: 302–307 (2005)

Introduction

A digital watermark is an imperceptible mark placed on multimedia content for a variety of applications including copyright protection, fingerprinting, broadcast monitoring, etc. In the recent years, digital watermarking has become an active area of research due to rapid development of multimedia networks and thus the need to prevent unauthorized duplication and distribution of multimedia content. In a watermarking system, the detection stage can be considered as the most crucial stage. Good detection schemes enable the recovery of a watermark with low probability of false detections. Two types of false detections are possible during the detection process. A false alarm occurs if a watermark is detected when no watermark has been embedded. On the other hand, a missed detection occurs when an existence of a watermark is rejected even though one is present. The complexity of the detector, the type of embedder used, and the characteristics of the watermark channel are among other things that influence the performance of the detection process.

Traditionally, watermark detection algorithms are based on computing correlation between the watermarked media and the watermark itself. Correlation detection is usually preferred because of its simplicity. Another advantage is that the detection can be 'blind', i.e., the original media is not required in the detection process. Blind detection is often more desirable and has wider applications.[1] However, correlation detection is known to be optimal only when the embedding process follows an additive rule and the medium is drawn from Gaussian distributions.[1]

More recent works on watermark detection are based on decision theory.[2–7] For this type of detection, an accurate model for the probability distribution function (PDF) of the original media is required. For example, in the works of Barni et al.[2] and Kwon et al.,[7] maximum likelihood (ML) detection schemes based on Bayes' decision theory are proposed for non-additive watermarks. A decision threshold is derived using the Neyman–Pearson criterion to minimize the missed detection probability subject to a given false alarm probability. Barni et al.[2] modeled magnitude of a set of discrete Fourier transform (DFT) coefficients using a Weibull PDF whereas Kwon et al.[7] modeled the discrete wavelet transform (DWT) coefficients using a Gaussian PDF. Experimental results in the context of robustness show that these schemes have better performance than the correlation detection. Moreover, blind detection is also possible by estimating the parameters of the PDF from the watermarked media.[4]

In this article, we propose a new ML detection model for image watermarking in DWT domain. It is based on modeling the DWT coefficients by a generalized Gaussian PDF. A decision threshold is also derived using the Neyman–Pearson criterion. The Laplacian and Gaussian PDFs are special cases of the generalized Gaussian PDF. Thus, the generalized Gaussian model is expected to result in a better watermark robustness as compared to the Laplacian and Gaussian models. Indeed, this result is shown to be generally true in our extensive experiments. The results in this article have

Original manuscript received June 14, 2004

†Corresponding Author: T. M. Ng, elengtm@nus.edu.sg

Supplemental Material— An Appendix can be found on the IS&T website (www.imaging.org) for a period of no less than two years from the date of publication.

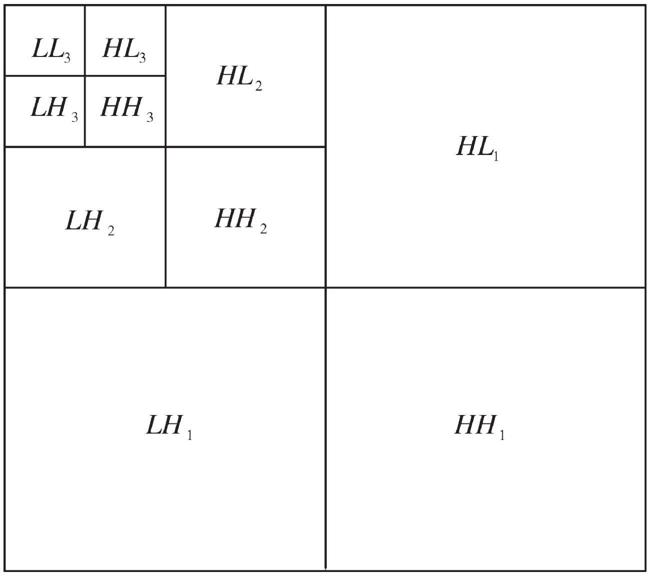

Figure 1. A DWT three-level pyramid decomposition of an image

been presented in part in Ref. 8. Proofs of some of the important results are given in *Appendix A, available as Supplemental Material*. The notation used is as follows. Non-bold letters are used to represent scalar quantities and functions, whereas bold letters are used for vectors. All vectors are real valued and expressed in column form.

Embedding Stage

In DWT domain watermarking, a watermark is embedded by modifying the DWT coefficients of a given image. Using DWT multiresolution decomposition,[9] an image can be separated into lower resolution subband (LL_1), and high resolution horizontal (HL_1), vertical (LH_1) and diagonal (HH_1) subbands. By repeating the process, a mutiple level pyramid decomposition can be obtained, see Fig. 1. For a watermark to be imperceptible, it is embedded in high resolution subbands where the human eye is less sensitive to noise.[10,11]

Let $\mathbf{x} = [x_1\ x_2\ .\ .\ .\ x_N]^T$ be the vector representing N DWT coefficients selected to embed a watermark $\mathbf{w} = [w_1\ w_2\ .\ .\ .\ w_N]^T$ chosen from a set M. The corresponding DWT coefficients of the watermarked image is represented as $\mathbf{y} = [y_1\ y_2\ .\ .\ .\ y_N]^T$. We view x_i, w_i and y_i as realizations of the random variables X_i, W_i and Y_i, respectively, for $i = 1, 2, \ldots, N$. The PDFs of X_i, W_i and Y_i are denoted as $f_{X_i}(x_i)$, $f_{W_i}(w_i)$ and $f_{Y_i}(y_i)$, respectively.

Embedding is usually done using either the additive rule as

$$y_i = x_i + \alpha_i w_i \tag{1}$$

or the non-additive rule as

$$y_i = x_i\,(1 + \alpha_i w_i), \tag{2}$$

for $i = 1, 2, \ldots, N$, where α_i is a positive scalar representing the embedding strength. The larger the embedding strength, the more robust is the watermark. However, this also means more distortion is being introduced into the image, thus the visual quality of the image may be affected. Therefore, it is important to tune the embedding strength to balance between robustness and imperceptibility of the watermark.

If the additive rule is used, then a correlation detector is usually employed to detect the watermark. As mentioned earlier, in correlation detection the presence of a watermark is determined by examining the correlation between the watermarked image and the watermark itself. The watermark is said to be detected if the correlation value is greater than a predefined threshold. The detection threshold has to be carefully selected to ensure accuracy in the detection process.[12]

On the other hand, non-additive rule usually works with an ML detector. Detection then amounts to thresholding a log likelihood function. In this case, the detection threshold and a correct PDF model for the DWT coefficients of the original image are required. The generalized Gaussian PDF is a commonly adopted model.[5] In the following sections, we consider embedding using the non-additive rule to derive an ML detection model based on the generalized Gaussian PDF.

Maximum Likelihood Detection

The components of the watermarks from the set M are assumed to be independent and uniformly distributed in $[-1, 1]$ so that

$$f_{\mathbf{W}}(\mathbf{w}) = \prod_{i=1}^{N} f_{W_i}(w_i) = \frac{1}{2^N}. \tag{3}$$

The set M is thus the N-dimensional space of $[-1, 1]$, written as $[-1, 1]^N$. Specifically, if $\mathbf{w}^* = [w_1^*\ w_2^*\ .\ .\ .\ w_N^*]^T$ is the embedded watermark, we can write $M = M_0 \cup M_1$, where $M_0 = \{\mathbf{w} : \mathbf{w} \neq \mathbf{w}^*\}$ and $M_1 = \{\mathbf{w}^*\}$. Note that $\mathbf{w} = \mathbf{0} = [0\ 0\ .\ .\ .\ 0]^T$ that corresponds to a non-marked image is already included in M_0.

In ML detection, two hypotheses are established as follows:

H_0: $\mathbf{y}$ is not marked with $\mathbf{w}^*$
H_1: $\mathbf{y}$ is marked with $\mathbf{w}^*$

The hypothesis H_1 is accepted or equivalently the watermark $\mathbf{w}^*$ is detected if

$$l(\mathbf{y}) = \frac{f_{\mathbf{Y}}(\mathbf{y} \mid M_1)}{f_{\mathbf{Y}}(\mathbf{y} \mid M_0)} > \lambda, \tag{4}$$

where $f_{\mathbf{Y}}(\mathbf{y} \mid M_j)$, $j = 0, 1$, are the conditional PDFs and λ is the decision threshold. The ratio $l(\mathbf{y})$ is called the likelihood ratio. The conditional PDF $f_{\mathbf{Y}}(\mathbf{y} \mid M_0)$ can be obtained as

$$f_{\mathbf{Y}}(\mathbf{y} \mid M_0) = \int_{[-1,1]^N} f_{\mathbf{Y}}(\mathbf{y} \mid \mathbf{w}) f_{\mathbf{W}}(\mathbf{w})\, d\mathbf{w}. \tag{5}$$

The Nth order integral in Eq. (5) should be taken over the set M_0 instead. But M_0 and $[-1\ 1]^N$ differ by a single point $\mathbf{w}^*$ which is of zero measure. Thus, integrating over $[-1, 1]^N$ is the same as integrating over M_0. Using Eq. (3) and under the assumption that the DWT coefficients are independent, we can express Eq. (5) as

$$f_{\mathbf{Y}}(\mathbf{y} \mid M_0) = \frac{1}{2^N} \prod_{i=1}^{N} \int_{-1}^{1} f_{\mathbf{Y_i}}(\mathbf{y_i} \mid \mathbf{w_i})\, dw_i. \tag{6}$$

In the non-additive rule, Eq. (2), the embedding strength α_i is set much lower than unity to make the watermark invisible. For small α_i, the integrals in Eq. (6) can be approximated so as to result in

$$f_{\mathbf{Y}}(\mathbf{y} \mid M_0) \approx f_{\mathbf{Y}}(\mathbf{y} \mid \mathbf{0}). \tag{7}$$

Barni et al.[2] derived this approximation for Weibull PDF, and it is also used by Kwon et al.[7] for Gaussian PDF. A general derivation of Eq. (7) which is valid for any PDF is given in *Appendix A, available as Supplemental Material*. Using Eq. (7) and the property of conditional independence of $Y_1, Y_2, \ldots, Y_N$, the likelihood ratio $l(\mathbf{y})$ can be expressed in terms of the PDFs of $X_1, X_2, \ldots, X_N$ as

$$l(\mathbf{y}) = \frac{\prod_{i=1}^{N} f_{Y_i}\left(y_i \mid w_i^*\right)}{\prod_{i=1}^{N} f_{Y_i}\left(y_i \mid 0\right)} = \frac{\prod_{i=1}^{N} \frac{1}{1+\alpha_i w_i^*} f_{X_i}\left(\frac{y_i}{1+\alpha_i w_i^*}\right)}{\prod_{i=1}^{N} f_{X_i}\left(y_i\right)}. \tag{8}$$

By taking the natural logarithm of the likelihood ratio, the decision rule Eq. (4), becomes

$$z(\mathbf{y}) = \sum_{i=1}^{N} \left[\ln f_{X_i}\left(\frac{y_i}{1+\alpha_i w_i^*}\right) - \ln f_{X_i}\left(y_i\right) \right] > \lambda', \tag{9}$$

where $\lambda' = \ln \lambda + \Sigma_{i=1}^{N} \ln(1 + \alpha_i w_i^*)$ is now the new decision threshold.

Neyman–Pearson Criterion

When a watermarked image is distorted, the missed detection probability P_{MD} can be much larger than the false alarm probability P_{FA}.[2] To overcome this problem, the Neyman–Pearson criterion can be used to obtain the decision threshold λ' in such a way that the missed detection probability is minimized subject to a specified false alarm probability, say P_{FA}^*. In view of Eq. (7), once P_{FA}^* has been fixed, λ' can be derived from

$$P_{FA}^* = P\left(z(\mathbf{y}) > \lambda' \mid M_0\right) = P\left(z(\mathbf{x}) > \lambda'\right) = \int_{\lambda'}^{\infty} f_{z(\mathbf{X})}\left(z(\mathbf{x})\right) dz(\mathbf{x}), \tag{10}$$

where

$$z(\mathbf{x}) = z(\mathbf{y})\,|_{\mathbf{y}=\mathbf{x}} = \sum_{i=1}^{N} \left[\ln f_{X_i}\left(\frac{x_i}{1+\alpha_i w_i^*}\right) - \ln f_{X_i}\left(x_i\right) \right]. \tag{11}$$

By the central limit theorem, the PDF of $z(\mathbf{X})$ can be assumed to be Gaussian with mean

$$\mu_{z(\mathbf{X})} = E\left[z(\mathbf{X})\right] = \sum_{i=1}^{N} E\left[\ln f_{X_i}\left(\frac{x_i}{1+\alpha_i w_i^*}\right) - \ln f_{X_i}\left(x_i\right) \right] \tag{12}$$

and variance

$$\sigma_{z(\mathbf{X})}^2 = V\left[z(\mathbf{X})\right] = \sum_{i=1}^{N} V\left[\ln f_{X_i}\left(\frac{x_i}{1+\alpha_i w_i^*}\right) - \ln f_{X_i}\left(x_i\right) \right]. \tag{13}$$

In this regard, Eq. (10) can be rewritten as

$$\begin{aligned} P_{FA}^* &= \int_{\lambda'}^{\infty} \frac{1}{\sqrt{2\pi\sigma_{z(\mathbf{X})}^2}} \exp\left(-\frac{\left(z(x) - \mu_{z(\mathbf{X})}\right)^2}{2\sigma_{z(\mathbf{X})}^2} \right) dz(\mathbf{x}) \\ &= \frac{1}{2} \operatorname{erfc}\left(\frac{\lambda' - \mu_{z(\mathbf{X})}}{\sqrt{2\sigma_{z(\mathbf{X})}^2}} \right), \end{aligned} \tag{14}$$

where erfc(·) is the complementary error function. Hence, the decision threshold λ' is obtained as

$$\lambda' = \operatorname{erfc}^{-1}\left(2P_{FA}^*\right)\sqrt{2\sigma_{z(\mathbf{X})}^2} + \mu_{z(\mathbf{X})}. \tag{15}$$

Probability Distribution Model

It is important to choose a PDF that matches the actual distribution of X_i to achieve optimum behavior of the ML detector. We propose modeling X_i as random variable having a generalized Gaussian PDF with zero mean. The Gaussian model by Kwon et al.[7] is also included here for comparison.

Generalized Gaussian Model

The zero mean generalized Gaussian PDF is expressed as

$$f_{X_i}\left(x_i\right) = a_i e^{-b_i^{\gamma_i} |x_i|^{\gamma_i}}, \tag{16}$$

where $\gamma_i > 0$ is the shape parameter of the distribution. The positive constant a_i and b_i are given as

$$a_i = \frac{b_i \gamma_i}{2\Gamma\left(1/\gamma_i\right)} \tag{17}$$

and

$$b_i = \frac{1}{\sigma_i} \sqrt{\frac{\Gamma\left(3/\gamma_i\right)}{\Gamma\left(1/\gamma_i\right)}}, \tag{18}$$

respectively, where σ_i^2 is the variance of the distribution and $\Gamma(u) = \int_0^{\infty} t^{u-1} e^{-t} dt$, $u > 0$, is the gamma function. Note that $\gamma_i = 1$ yields the Laplacian PDF and $\gamma_i = 2$ yields the Gaussian PDF.

Substituting Eqs. (16) and (18) in Eq. (9), we obtain the decision rule as

$$z(\mathbf{y}) = \sum_{i=1}^{N} |y_i|^{\gamma_i} \left[\frac{1}{\sigma_i} \sqrt{\frac{\Gamma\left(3/\gamma_i\right)}{\Gamma\left(1/\gamma_i\right)}} \right]^{\gamma_i} \left[1 - \frac{1}{\left|1+\alpha_i w_i^*\right|^{\gamma_i}} \right] > \lambda'_{gg}. \tag{19}$$

In view of Eq. (15), mean and variance of $z(\mathbf{X}) = z(\mathbf{Y})\,|_{\mathbf{Y}=\mathbf{X}}$ are required to obtain λ'_{gg}, the decision threshold for the generalized Gaussian case. Equivalently, we need to find the mean and variance of $|X_i|^{\gamma_i}$. It is shown in *Appendix A, available as Supplemental Material* that

$$E\left[\left|X_i\right|^c\right] = \sigma_i^c \frac{\Gamma\left((c+1)/\gamma_i\right)}{\Gamma^{1-c/2}\left(1/\gamma_i\right)\Gamma^{c/2}\left(3/\gamma_i\right)}, \tag{20}$$

where c is a constant. In particular, when c is a positive even integer, the even moments of X_i are given by Eq. (20). When $c = \gamma_i$, it follows from the property of gamma function that $\Gamma((c+1)/\gamma_i) = \Gamma(1+1/\gamma_i) = \Gamma(1/\gamma_i)/\gamma_i$. Substituting this into Eq. (20) yields

$$E\left[|X_i|^{\gamma_i}\right] = \frac{\sigma_i^{\gamma_i}}{\gamma_i}\left[\frac{\Gamma(1/\gamma_i)}{\Gamma(3/\gamma_i)}\right]^{\gamma_i/2}. \tag{21}$$

Since $V[|X_i|^{\gamma_i}] = E[|X_i|^{2\gamma_i}] - (E[|X_i|^{\gamma_i}])^2$, it follows from Eq. (20) that

$$V\left(|X_i|^{\gamma_i}\right) = \frac{\sigma_i^{2\gamma_i}}{\gamma_i}\left[\frac{\Gamma(1/\gamma_i)}{\Gamma(3/\gamma_i)}\right]^{\gamma_i}. \tag{22}$$

With Eqs. (21) and (22), it is straightforward to obtain

$$\mu_{z(\mathbf{X})} = \sum_{i=1}^{N} \frac{1}{\gamma_i}\left[1 - \frac{1}{\left|1+\alpha_i w_i^*\right|^{\gamma_i}}\right] \tag{23}$$

and

$$\sigma_{z(\mathbf{X})}^2 = \sum_{i=1}^{N} \frac{1}{\gamma_i}\left[1 - \frac{1}{\left|1+\alpha_i w_i^*\right|^{\gamma_i}}\right]^2. \tag{24}$$

In Eq. (19), the variance σ_i^2 and shape parameter γ_i have to be estimated from the DWT coefficients of either the original image or the watermarked image. As the embedding is done in an imperceptible manner, estimation using the DWT coefficients of the watermarked image should be close to that of the original image.[4] Let B be the DWT subband containing x_i and having N_B coefficients. All coefficients in B are assumed to be identically distributed, i.e., they have identical PDF. Then an unbiased estimator of σ_i^2 is given as

$$\hat{\sigma}_i^2 = \frac{1}{N_B - 1}\sum_{y\in B} y^2, \tag{25}$$

where y is the corresponding DWT coefficient of the watermarked image (possibly distorted) in B. To obtain an estimator for γ_i, we express Eq. (20) as

$$\frac{\sigma_i^{2c}}{E^2\left[|X_i|^c\right]} = \frac{\Gamma^{2-c}(1/\gamma_i)\Gamma^c(3/\gamma_i)}{\Gamma^2((c+1)/\gamma_i)}. \tag{26}$$

Note that for a fixed $c \neq 2$, the right-hand side of Eq. (26) is solely a function of γ_i. Thus, by defining $r(\gamma_i) = \sigma_i^{2c}/E^2[|X_i|^c]$, we can estimate γ_i as

$$\hat{\gamma}_i = r^{-1}\left(\frac{\hat{\sigma}_i^{2c}}{\left[\frac{1}{N_B}\sum_{y\in B}|y|^c\right]^2}\right). \tag{27}$$

The case when $c = 1$ is first given by Mallat,[9] and is also studied by Sharifi and Leon–Garcia[13] who referred to r as the generalized Gaussian ratio function.

One way to solve Eq. (27) is to approximate the inverse of the function r using any of the well-known function interpolation methods.[14] The knowledge of the range of r would be useful to achieve the desired accuracy in the interpolation process. When $c = 1$, we show in *Appendix A, available as Supplemental Material* that r is a strictly decreasing function of γ_i with

$$\lim_{\gamma_i \to 0^+} r(\gamma_i) = +\infty \tag{28}$$

and,

$$\lim_{\gamma_i \to +\infty} r(\gamma_i) = 4/3. \tag{29}$$

For high resolution DWT subbands, it is sufficient to apply interpolation based on $0.1 \le \gamma_i \le 3$.[4]

Gaussian Model

If X_i is modeled as a Gausian random variable with PDF

$$f_{X_i}(x_i) = \frac{1}{\sigma_i\sqrt{2\pi}} e^{-\frac{(x_i-\mu_i)^2}{2\sigma_i^2}}, \tag{30}$$

where μ_i is the mean and σ_i is the variance, then the decision rule becomes

$$z(\mathbf{y}) = \sum_{i=1}^{N} \frac{1}{2\sigma_i^2}\left[(y_i-\mu_i)^2 - \left(\frac{y_i}{1+\alpha_i w_i^*} - \mu_i\right)^2\right] > \lambda'_g. \tag{31}$$

By noting that the central moments of X_i[15] are given as

$$E\left[(X_i-\mu_i)^n\right] = \begin{cases} 1\cdot 3\cdots(n-1)\sigma_i^n & n = 2k \\ 0 & n = 2k+1 \end{cases}, \tag{32}$$

it is straightforward to show that

$$\mu_{z(\mathbf{X})} = \sum_{i=1}^{N}\left\{\frac{1}{2}\left[1 - \frac{1}{(1+\alpha_i w_i^*)^2}\right] - \frac{1}{2(1+\alpha_i w_i^*)^2}\left(\frac{\mu_i\alpha_i w_i^*}{\sigma_i}\right)^2\right\} \tag{33}$$

and

$$\sigma_{z(\mathbf{X})}^2 = \sum_{i=1}^{N}\left\{\frac{1}{2}\left[1 - \frac{1}{(1+\alpha_i w_i^*)^2}\right]^2 + \frac{1}{(1+\alpha_i w_i^*)^4}\left(\frac{\mu_i\alpha_i w_i^*}{\sigma_i}\right)^2\right\}, \tag{34}$$

as required to form the decision threshold λ'_g. When $\mu_i = 0$, we see that Eqs. (33) and (34) reduce to Eqs. (23) and (24), respectively, with $\gamma_i = 2$.

Experimental Results

The proposed ML detector is tested using the 512×512 images shown in Fig. 2. During the watermark embedding stage, each image is first transformed by DWT using a Daubechies filter to obtain a three-level DWT decomposition. For simplicity, we embed to all the DWT

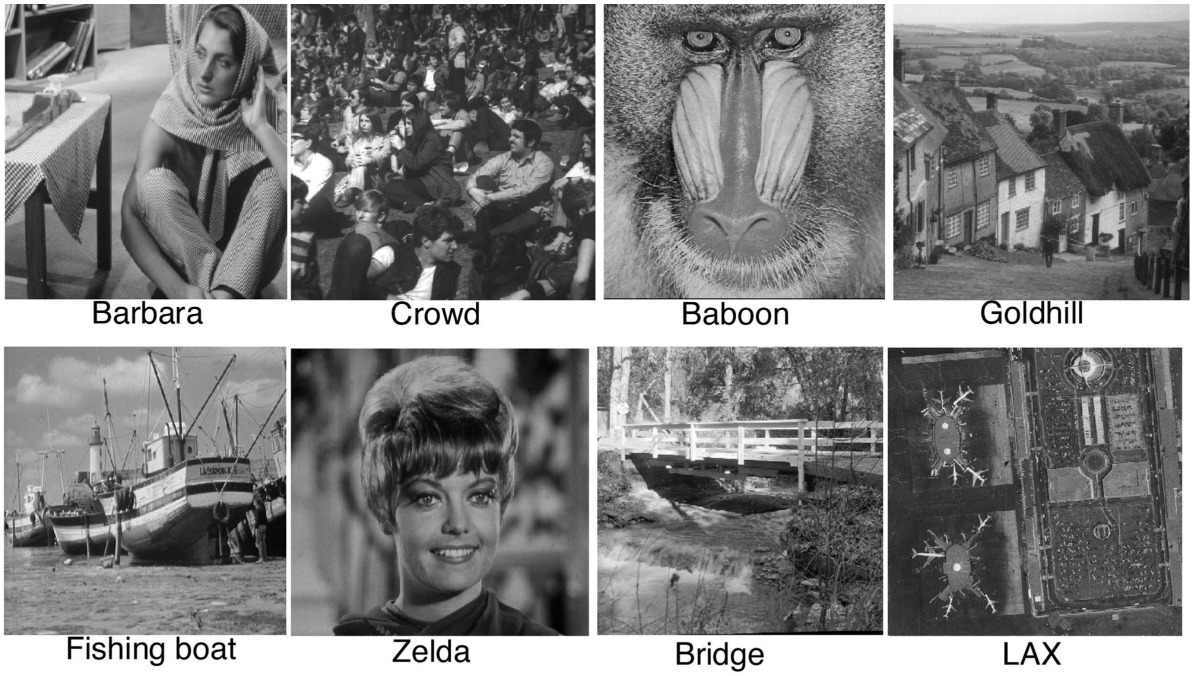

Figure 2. Test Images

TABLE I. Watermark Embedding Strength for Images

Image	α
Barbara	0.185
Crowd	0.150
Baboon	0.170
Goldhill	0.205
Fishing boat	0.175
Zelda	0.215
Bridge	0.155
LAX	0.190

TABLE II. Percentage of Successful Detections Under JPEG Compression

Image	Generalized Gaussian	Gaussian	Gaussian (non-zero mean)	Laplacian
Barbara	100.00	75.66	75.66	99.13
Crowd	100.00	98.25	98.30	99.98
Baboon	100.00	99.95	99.95	100.00
Goldhill	100.00	91.26	91.28	99.83
Fishing boat	99.93	85.10	85.13	98.51
Zelda	100.00	90.33	90.33	99.65
Bridge	100.00	97.63	97.63	100.00
LAX	100.00	81.11	81.13	99.71

coefficients in LH_3, HL_3 and HH_3 subbands. Embedding can also be restricted to say the first 5000 coefficients with the largest magnitude in these subbands.[7] This would minimize the noise introduced by the watermark in the image.

A constant embedding strength α is used for all the DWT coefficients in the three subbands. Table I shows the values of α chosen so that the peak signal to noise ratio (PSNR)[16] of each watermarked image is about 45 dB. A PSNR of 40 dB and above is usually considered as good image quality. The steps for testing the robustness of the proposed ML detector are summarized as follows:

1. Select an image and obtain its DWT.
2. Generate a set M' containing 100 watermarks.
3. Select a watermark from M' and embed to the subbands LH_3, HL_3 and HH_3 of the image.
4. Distort the watermarked image using a standard image processing operation, e.g., JPEG compression.
5. Compute $\hat{\sigma}_i^2$ and $\hat{\gamma}_i$ using Eqs. (25) and (27), respectively, from the distorted watermarked image.
6. Compute the decision threshold λ'_{gg} using Eq. (15) with $\mu_z(\mathbf{x})$ and $\sigma^2_{z(\mathbf{x})}$ given by Eqs. (23) and (24), respectively, and $P^*_{FA} = 10^{-9}$ or $\mathrm{erfc}^{-1}(2P^*_{FA}) = 4.24$.
7. Compute $z(\tilde{\mathbf{y}})$ as in Eq. (19) ($\tilde{\mathbf{y}}$ being the distorted version of $\mathbf{y}$) for all the watermarks in M'_0, and then compare them with λ'_{gg}.
8. If $z(\tilde{\mathbf{y}}) > \lambda'_{gg}$ for the embedded watermark but not for any other watermarks in M'_0, then the detection is said to be successful. Otherwise it is a failure.

For each standard image processing operation, steps 1–8 are repeated for 10,000 trials for each image. A different set M'_0 is used in each trial. The percentage of successful detections are recorded for each image.

Tables II through V shows a set of the results obtained. The generalized Gaussian model is compared with the Gaussian and Laplacian models. Similar results can also be found in Ref. 8 with $P^*_{FA} = 10^{-6}$. Here, the non-zero mean Gaussian model is also included in the comparison. In Table II, the watermarked images are compressed by JPEG with a 50% quality factor. In Table III, the watermarked images are low pass filtered using a 4×4 spatial filter. In Table IV, the pixels of the watermarked images are up-scaled by a factor of 3. Lastly, in Table V, the watermarked images are corrupted by zero mean Gaussian noise of variance 0.5. Except for the images 'Barbara', 'Crowd' and 'Bridge' in

TABLE III. Percentage of Successful Detections Under Low Pass Filtering

Image	Generalized Gaussian	Gaussian	Gaussian (non-zero mean)	Laplacian
Barbara	33.09	54.66	54.68	68.37
Crowd	65.21	75.08	75.08	55.40
Baboon	91.40	88.31	88.40	90.10
Goldhill	97.80	70.34	70.34	90.36
Fishing boat	90.94	47.84	47.87	45.90
Zelda	95.51	66.33	66.25	79.33
Bridge	41.07	59.21	59.23	86.35
LAX	67.32	31.53	31.51	58.55

TABLE IV. Percentage of Successful Detections Under Scaling

Image	Generalized Gaussian	Gaussian	Gaussian (non-zero mean)	Laplacian
Barbara	99.90	80.41	80.29	98.93
Crowd	99.93	95.82	95.84	99.89
Baboon	100.00	99.80	99.80	100.00
Goldhill	100.00	86.20	86.31	99.43
Fishing boat	99.94	72.30	72.61	95.17
Zelda	100.00	93.03	93.11	99.92
Bridge	100.00	95.53	95.53	100.00
LAX	100.00	80.73	80.91	100.00

Table III, it is clear from the results that the generalized Gaussian model yields better detection. Also note that the non-zero mean Gaussian model offers only little improvement over the zero mean Gaussian model. This is somewhat to be expected insofar as the mean of the DWT coefficients in the subbands is close to zero.

Conclusion

In this article, we have proposed an ML detection model for image watermarking in DWT domain. A generalized Gaussian PDF is used to model the distribution of the DWT coefficients. Based on the work of Barni et al.,[2] we explicitly derived a decision threshold for the proposed model using the Neyman–Pearson criterion. Our extensive experiments revealed that the generalized Gaussian PDF results in a better detection performance as compared to the Gaussian and Laplacian PDFs. The general idea presented here is also applicable to watermark detection in other forms of multimedia data and forms the basis of on-going research.

TABLE V. Percentage of Successful Detections Under Gaussian Noise

Image	Generalized Gaussian	Gaussian	Gaussian (non-zero mean)	Laplacian
Barbara	100.00	97.10	97.10	100.00
Crowd	100.00	99.70	99.79	100.00
Baboon	96.22	88.76	88.64	94.48
Goldhill	99.19	95.23	95.37	98.81
Fishing boat	89.13	51.12	51.28	62.32
Zelda	99.82	94.90	94.92	98.91
Bridge	100.00	99.63	99.66	100.00
LAX	99.28	96.70	96.77	99.08

References

1. I. J. Cox, M. L. Miller and J. A. Bloom, *Digital Watermarking*, Morgan Kaufmann Publishers, San Francisco, 2002.
2. M. Barni, F. Bartolini, A. De Rosa, and A. Piva, A new decoder for the optimum recovery of nonadditive watermarks, *IEEE Trans. Image Processing* **10**(5), 755–766 (2001).
3. T. P.–C. Chen and T. Chen, A framework for optimal blind watermark detection, *Proc. ACM Multimedia 2001*, *Workshop on Multimedia and Security: New Challenges*, ACM, Ottawa, Canada, 2001.
4. Q. Cheng and T. S. Huang, Blind digital watermarking for images and videos and performance analysis, *IEEE Int'l. Conf. Multimedia and Expo,* **1,** 389–392 (2000).
5. Q. Cheng and T. S. Huang, Robust optimum detection of transform domain multiplicative watermarks, *IEEE Trans. Signal Processing,* **51**(4), 906–924 (2003).
6. J. R. Hernández and F. Pérez–González, Statistical analysis of watermarking schemes for copyright protection of images, *Proc. IEEE*, **87**(7), 1142–1166 (1999).
7. S. G. Kwon, S.-H. Lee, K.-K. Kwon, K.-R. Kwon, and K.-I. Lee, Watermark detection algorithm using statistical decision theory, *Proc. IEEE Int. Conf. on Multimedia and Expo* **1,** 561–564 (2002).
8. T. M. Ng and H. K. Garg, Wavelet domain watermarking using maximum-likelihood detection, *Proc. SPIE*, **5306,** 816–826 (2004).
9. S. G. Mallat, A theory for multiresolution signal decomposition: the wavelet representation, *IEEE Trans. Pattern Analysis and Machine Intelligence* **11**(7), 674–693 (1989).
10. G. C. Langelaar, I. Setyawan and R. L. Lagendijk, Watermarking digital image video data: a state-of-art overview, *IEEE Signal Processing Magazine,* 20–46 (Sept. 2000).
11. X.-G. Xia, C. G. Boncelet and G. R. Acre, Wavelet transform based watermark for digital images, *Opt. Express* **3**(12), 497–511 (1998).
12. A. Piva, M. Barni, F. Bartolini, and V. Cappellini, Threshold selection for correlation-based watermark detection, L'Aquila, Italy, 1998.
13. K. Sharifi and A. Leon–Garcia, Estimation of shape parameter for generalized Gaussian distributions in subband decompositions of video, *IEEE Trans. Circuits and Systems for Video Tech.* **5**(1), 52–56 (1999).
14. D. Kincaid and W. Cheney, *Numerical Analysis*, 2nd ed., Brooks/Cole Pacific Grove, CA, 1996.
15. A. Papoulis, Probability, *Random Variables, and Stochastic Processes*, McGraw-Hill, Inc., New York, NY, 1991, p. 110.
16. M. Kutter and F. A. P. Petitcolas, A fair benchmark for image watermarking systems, *Proc. SPIE* **3657,** 226–239 (1999).
17. S. G. Krantz, *Handbook of Complex Variables*, Birkhäuser, Boston, 1999, p. 156.